Original Research Article

Isotopic Effects on the Structure and Spectroscopy of Thioformaldehyde, Dihydrogen and Water

John Paul Shinggu * ⓘD, Emmanuel Edet Etim ⓘD, Alfred Ikpi Onen

Department of Chemical Sciences, Federal University Wukari, Taraba State, Nigeria

ARTICLE INFO

## ABSTRACT

This research presents a comprehensive computational study of deuterated molecular species, namely SCH_2, H_2, and H_2O, focusing on the impact of deuteration on their spectroscopic properties. Utilizing advanced quantum chemical methods, including MP2/cc-pVDZ, MP2/6-311*, G4, W2U, and CCSD/cc-pVDZ, the molecular geometries of the deuterated species were optimized to investigate their dipole moments, vibrational frequencies, and rotational constants. The vibrational frequencies provided insights into molecular vibrations, while the rotational constants described rotational motion. In addition, bond lengths and bond angles were computed to understand the molecular structure and bonding patterns. Subsequently, dipole moments were analyzed to assess polarity and charge distribution. The results revealed significant alterations in the spectroscopic properties due to deuteration, leaving the structural properties unaffected.

GRAPHICAL ABSTRACT
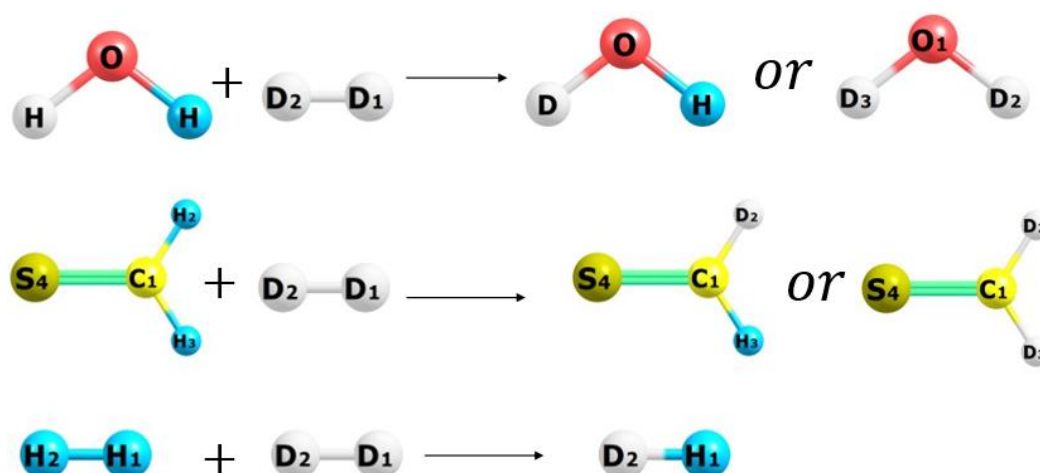
* Corresponding author: Shinggu, John Paul
✉ E-mail: johnshinggu@gmail.com

Introduction

Deuterium, an isotope of hydrogen, exerts a notable impact on molecules due to its increased mass compared to protium, the more common hydrogen isotope. This isotopic substitution changes molecular properties and reactivity [1]. Deuterium causes a redshift in vibrational frequencies and alters reaction rates through kinetic isotope effects and hydrogen bonding behavior [2]. Deuterium labeling is widely used in research to study molecular pathways, interactions, and mechanisms [3]. Deuterium's distinctive presence has enabled its detection through spectroscopic analysis, providing a window into the conditions of interstellar regions, star formation processes, and the origin of planets [4].

In astrophysics, deuterated molecules provide valuable insights into interstellar chemistry, while in astrobiology, they offer clues about potential extraterrestrial life [5]. The presence of deuterium in molecules significantly shapes our understanding of molecular behavior, from fundamental chemical processes to its role in the interstellar medium.

Deuterium fractionation is a well-known mechanism in the thick interstellar medium that may occur both in the gas phase and on the surfaces of dust particles [6,7]. Due to this mechanism, the deuterated isotopic interstellar molecular species can have abundances much greater than the D/H elemental abundance ratio [8]. As with HDCS [9] and CH_2DOH, the great efficiency of deuterium fractionation allows deuterated species to gain 30-40% of their parent species' abundance [10]. As a result, deuterated isotopologues of a wide range of interstellar compounds considerably boost the spectrum variety. Hence, it is crucial to identify these isotopologues using astronomy to learn more about their molecular creation processes and how deuterium fractionation works and assign unidentified features in line surveys [6].

Studying isotopic abundance variations in diverse settings is an essential aspect of astrochemistry. Deuterium stands out among the visible isotopes since it is the most common rare isotope of all the elements' isotopic forms. Because the reservoir is considered primordial, astronomers are perplexed by the astral generation of tiny deuterium atoms [11]. The significant relative mass differential between hydrogen and deuterium causes the two species' distinct chemical sensitivities. This has the unintended consequence of considerably fractionating deuterium in cold clouds, where its concentration can reach three orders of magnitude higher than hydrogen. As a result, molecules with isotopically substituted deuterium atoms are easily identified. A modest number of observations of a molecule in different isotopic states enables a unique assessment of its astrochemistry [12].

Snell and Wootten (1979) revealed that the DNC/HNC abundance ratio is significantly temperature dependent. The bulk of molecular ions are destroyed due to electron recombination. Previously, it was thought that this predominated H_3^+ destruction, allowing limits on electron abundance to be established based on estimations of the H_2D^+/H_3^+ abundance ratio obtained from DCO^+/HCO^+ abundant ratios [13,14].

The isotopic abundance of hydrogen and its isotopes varies in different environments [15]. For instance, the isotopic composition of hydrogen in water can provide insights into the sources and history of water samples. Additionally, the relative abundances of hydrogen isotopes in certain molecules can help scientists trace chemical reactions, investigate metabolic pathways, and study ancient climates by analyzing ice cores [16]

Computational Methods

The molecular geometries of SCH_2, H_2, and H_2O were optimized for all the deuterated species using the mentioned methods: MP2/cc-pVDZ, MP2/6-311*, G4, W2U, and CCSD/cc-pVDZ. The optimization process involved finding the most stable arrangements of atoms by minimizing the potential energy. Subsequently, using the same methods, frequency calculations were carried out to obtain vibrational frequencies and rotational constants for each deuterated molecule. The vibrational frequencies provided insights into the molecular vibrations, while the rotational constants described the rotational motion of the molecules. Bond lengths and angles were also computed from the optimized molecular geometries to understand the molecular structure and bonding patterns. Finally, dipole moments were computed to analyze molecules' polarity and charge distribution. The CCSD/cc-pVDZ method refers to the Coupled-Cluster Singles and Doubles calculation using the correlation-consistent polarized valence double-zeta basis set [17], which is a quantum chemical approach for accurately modeling electronic interactions in molecules. MP2/cc-pVDZ signifies the Second-Order Møller-Plesset Perturbation Theory calculation with the same basis set, an approximate post-Hartree-Fock method capturing electron correlation effects [18]. MP2-6-311* represents the MP2 method augmented with a more significant 6-311G(d,p) basis set, incorporating more basis functions for improved accuracy [19]. W2U denotes the "W2U" composite method, a combination of explicitly correlated W2-F12 and the correlation-consistent polarized valence basis set, aiming for high-precision energy calculations [20]. Lastly, G4 refers to the Gaussian-4 method, a composite approach integrating density functional theory,

MP2, and CCSD(T) methods with the cc-pVnZ basis sets to achieve highly accurate thermochemical properties predictions for molecules [21]. Using the Moller-Plesset second-order perturbation theory approach (MP2), the 6-311* basis set and the correlation-consistent Polarized Valence Double Zeta (CC-Pvdz) basis set were used. In addition to the approaches described above, the coupled cluster approach was used at the correlation-consistent Polarized Valence Double Zeta (CC-Pvdz) basis set [11]. To predict suitable proton affinities for all of the systems tested, compound models such as the Gaussian theory (G4) and the Weizmann theory (W2U) were used [22,23]. All the results obtained from the above methods were compared with their experimental values obtained from the NIST Chemistry Webbook.

Results and discussion

Deuterium fractionation in the dense interstellar medium has long captivated the attention of astrophysicists and chemists alike, as it plays a pivotal role in enhancing the abundance of deuterated isotopic interstellar molecular species beyond the D/H elemental abundance ratio. This research extensively investigates deuterated molecules, explicitly focusing on H_2, H_2O, and SCH_2, employing advanced quantum chemical methods. The deuterium isotopologues of these species hold significant implications in various scientific fields, including atmospheric chemistry, combustion processes, and astrochemistry.
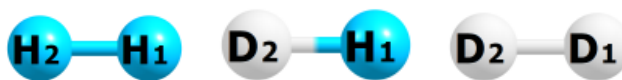
Hydrogen H_2

Structural Parameters

Figure 1. Optimized geometries of H_2, DH and D_2.

Table 1. Bond length values of H_2, DH and D_2

Method	Bond Lengths (Å) H_2, DH and D_2		
	R(H1-H2)	R(H1-D2)	R(D1-D2)
Experimental	0.740	0.741	0.741
G4	0.740	0.740	0.740
MP2/cc-pvdz	0.754	0.754	0.754
CCSD/ cc-pvdz	0.761	0.761	0.761
W2U	0.742	0.742	0.721
MP2/6-311*	0.738	0.738	0.738

Rotational constant values for H_2, DH and D_2

The rotational constants for H_2, DH, and D_2 are 1824.327 GHz, 1368.702 GHz, and 912.676 GHz, respectively. The rotational constant of a diatomic molecule is inversely proportional to its moment of inertia, which, in turn, depends on the reduced mass of the molecule. In this case, H_2 has the highest rotational constant, followed by DH and D_2. This is because the reduced mass of H_2 is the smallest among the three, resulting in a higher rotational constant. DH, with a slightly heavier reduced mass than H_2, exhibits an intermediate rotational constant. D_2, the heaviest with the most enormous reduced mass, shows the lowest rotational constant. Thus, the comparison demonstrates that the rotational behavior of these molecules is influenced by the masses of their constituent atoms, with lighter isotopes yielding higher rotational constants.

Table 2. Rotational constants of H_2, DH, and D_2

Method		Rotational Constants (Ghz)		
		A	B	C
H_2	Experimental	0.000	1824.327	1824.327
	G4	0.000	1831.465	1831.465
	MP2/cc-pvdz	0.000	1831.465	1831.465
	CCSD/cc-pvdz	0.000	1831.465	1831.465
	W2U	0.000	1831.465	1831.465
	MP2/6-311*	0.000	1831.465	1831.465
DH	Experimental	0.000	1368.702	1368.702
	G4	0.000	1819.134	1819.134
	MP2/cc-pvdz	0.000	1322.133	1322.133
	CCSD/ cc-pvdz	0.000	1299.553	1299.553
	W2U	0.000	1823.456	1823.456
	MP2/6-311*	0.000	1845.638	1845.638
D_2	Experimental	0.000	912.676	912.676
	G4	0.000	1819.134	1819.134
	MP2/cc-pvdz	0.000	881.874	881.874
	CCSD/ cc-pvdz	0.000	866.813	866.813
	W2U	0.000	1891.245	1891.245
	MP2/6-311*	0.000	1845.638	1845.638

Dipole moment

Due to their linear and symmetrical molecular structures, H_2, DH, and D_2 have no dipole moment. In H_2 (hydrogen gas), the two hydrogen atoms are connected by a covalent bond, forming a linear molecule. Since both hydrogen atoms are identical and have the same electronegativity, the electron density is evenly distributed, resulting in a symmetrical charge distribution and canceling any dipole moment. Similarly, in deuterium-hydrogen (DH) and deuterium gas (D_2), the linear arrangement of the atoms and the identical electronegativity of hydrogen and deuterium lead to a symmetrical charge distribution and no net dipole moment. These molecules' positive and negative charges are perfectly balanced, resulting in a zero dipole moment, making them nonpolar.

Vibrational Frequencies

The vibrational frequencies given off by H_2, DH, and D_2 are 4161.2 cm^{-1}, 3632 cm^{-1}, and 2993.0 cm^{-1}, respectively. These frequencies correspond to the stretching and bending motions of each molecule's hydrogen-hydrogen (H-H) bonds. The decrease in frequency from H_2 to D can be attributed to the difference in masses; deuterium (D) is twice as heavy as hydrogen (H), resulting in a lower vibrational frequency due to a higher reduced mass. Similarly, DH, with an intermediate mass between H_2 and D_2, exhibits a frequency between the other two. This comparison illustrates the inverse relationship between vibrational frequencies and the masses of the atoms involved, highlighting how isotopic substitutions affect molecular vibrations.

Table 3. Dipole Moment values for H_2, DH and D_2

Method	Dipole Moment (Debye) DH	Dipole Moment (Debye) H_2	Dipole Moment (Debye) D_2
Experimental	0.000	0.000	0.000
G4	0.000	0.000	0.000
MP2/cc-pvdz	0.000	0.000	0.000
CCSD/ cc-pvdz	0.000	0.000	0.000
W2U	0.000	0.000	0.000
MP2/6-311*	0.000	0.000	0.000

Table 4. Vibrational Frequency values of H_2, DH and D_2

	Vibrational Frequencies (cm^{-1})					
	Experimental	G4	CCSD/CC-PVDZ	W2U	MP2/6-311*	MP2/CC-PVDZ
D_2	2993.0	3037.9379	3871.5821	3217.4314	3089.1342	3161.8452
DH	3632.2	3743.6711	3665.7125	3715.9991	3285.2125	3836.6352
H_2	4161.2	4466.4384	4382.8819	4434.4137	4491.5425	4501.2610

Water H_2O

Structural Parameters

H_2O, HDO, and D_2O have similar bond lengths and bond angles despite having different isotopes of hydrogen (H and D) because the electronic structure of oxygen primarily governs the bonding in water molecules. The bond length

and bond angle in a water molecule are mainly determined by the arrangement of its electrons and the hybridization of the oxygen atom's orbitals. Oxygen has six valence electrons, and in a water molecule, it forms two sigma bonds with the two hydrogen atoms. The electronic configuration and hybridization of oxygen remain nearly the same regardless of whether the hydrogen atoms are H, D, or a combination of both.

Since the electronic structure of oxygen remains constant, the bonding orbitals and bond angles in H_2O, HDO, and D_2O are nearly identical. As a result, the bond lengths are very similar (0.958 Å for H_2O, 0.956 Å for HDO, and 0.956 Å for D_2O) because the spatial arrangement of the atoms is not significantly affected by the substitution of hydrogen with deuterium. The slight difference in bond lengths can be attributed to subtle changes in the atomic masses. However, overall, the similarity in the bond angles and lengths is primarily due to the consistent electronic configuration and hybridization of the oxygen atom in all three water isotopologues.
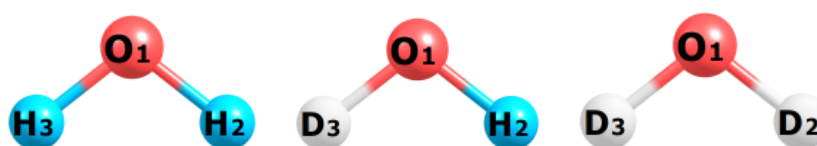

Figure 2. Optimized geometries of H_2O, DHO, and D_2O

Table 5. Bond Lengths and Bond Angles of H_2O, DHO and D_2O

Bond lengths, R (Å) and Bond angles, A (°) of H_2O, DHO and D_2O						
		Experimental	G4	CCSD/CC-PVD	W2U	MP2/6-311*	MP2/CC-PVDZ
	R(O1-H2)	0.958	0.962	0.965	0.967	0.959	0.9643
H_2O	R(O1-H3)	0.958	0.962	0.965	0.967	0.959	0.9643
	A(H2-O1-H3)	104.4776	103.7	102.18	103.8	103.5	101.94
	R(O1-H2)	0.956	0.962	0.965	0.967	0.959	0.9643
DHO	R(O2-D3)	0.956	0.962	0.965	0.967	0.959	0.9643
	A(H2-O1-D3)	104.4776	103.7	102.18	103.8	103.5	101.94
	R(O1-D2)	0.956	0.962	0.965	0.967	0.959	0.9643
D_2O	R(O1-D3)	0.956	0.962	0.965	0.967	0.959	0.9643
	A(D2-O1-D3)	104.4776	103.7	102.18	103.8	103.5	101.94

Rotational Constants

The rotational constants of H_2O, HDO, and D_2O differ due to the isotopic substitutions of hydrogen with deuterium. The rotational constant of a diatomic molecule is inversely proportional to its moment of inertia, which, in turn, depends on the reduced mass of the molecule. When deuterium replaces hydrogen, the molecular mass increases, resulting in a

higher reduced mass for HDO and D_2O compared to H_2O. Consequently, the moment of inertia increases for HDO and D_2O, leading to lower rotational constants. Thus, H_2O, the lightest isotopologue, has the highest rotational constants (835.73144 GHz, 435.05882 GHz, and 278.35730 GHz for the three rotational axes). In comparison, the rotational constants decrease for HDO (701.93 GHz, 272.90 GHz, and 192.06 GHz) and further decrease for D_2O (462.279 GHz, 218.038 GHz, and 145.258 GHz) due to the increasing masses of deuterium, highlighting the impact of isotopic substitutions on the rotational behavior of these water isotopologues.

Table 6. Rotational constant values for H_2O, HDO, and D_2O

Method	Rotational Constants (Ghz)		
	A	B	C
H_2O			
Experimental	835.73144	435.05882	278.35730
G4	794.68	434.84	281.05
MP2/cc-pvdz	765.609	446.773	282.133
CCSD/cc-pvdz	768.697	444.795	281.759
W2U	791.443	421.436	286.409
MP2/6-311*	786.787	449.781	286.181
DHO			
Experimental	701.93	272.90	192.06
G4	673.52	271.07	193.28
MP2/cc-pvdz	654.972	275.907	194.130
CCSD/ cc-pvdz	656.887	275.010	193.852
W2U	657.212	276.38	194.051
MP2/6-311*	670.577	278.781	192.542
D_2O			
Experimental	462.279	218.038	145.258
G4	442.080	217.590	145.820
MP2/cc-pvdz	425.848	223.581	146.608
CCSD/ cc-pvdz	427.702	222.538	146.377
W2U	439.242	226.452	147.348
MP2/6-311*	437.593	225.120	148.648

Dipole Moments

The dipole moments of H_2O, HDO, and D_2O are 1.860 Debye, 1.850 Debye, and 1.850 Debye, respectively. The molecular geometry and electron density distribution within these water isotopologues can explain the similarity in their dipole moments. In all three molecules, the central oxygen atom is highly electronegative, causing it to attract the shared electrons in the O-H bond toward itself. This creates a significant partial negative charge on the oxygen atom and a partial positive charge on the hydrogen or deuterium atoms.

The dipole moment of a molecule is the product of the charge and the distance between the charges, so even though HDO and D2O have heavier isotopes (deuterium) compared to H_2O (hydrogen), the difference in dipole moments is minimal because the change in charge distribution upon isotopic substitution is relatively tiny. The geometry of the water molecule, with the oxygen atom at the center and the hydrogen/deuterium atoms forming a bent shape, leads to a comparable arrangement of the

partial charges in H_2O, HDO, and D_2O. As a result, their dipole moments are similar despite the isotopic differences, making them all highly polar molecules with only marginal variation in their overall polarity.

Vibrational Frequency

The vibrational frequencies of H_2O, DHO, and D_2O exhibit interesting patterns due to the isotopic substitutions of hydrogen with deuterium. These frequencies represent the energies required for the molecules to undergo different vibrational modes, such as stretching and bending motions. When comparing the vibrational frequencies, several trends become apparent.

The vibrational frequencies of H_2O, DHO and D_2O can be seen in the table below. For H_2O, the vibrational frequencies are 3657.0 cm^{-1} (stretching), 1595.0 cm^{-1} (bending, in-plane), and 3756.0 cm^{-1} (bending, out-of-plane). As we move to DHO, which contains one deuterium (D) and one hydrogen (H), the vibrational frequencies shift to 3707.0 cm^{-1} (stretching), 2727.0 cm^{-1} (bending, in-plane), and 1402.0 cm^{-1} (bending, out-of-plane). Notably, DHO has higher vibrational frequencies compared to H_2O,

particularly for the stretching and bending in-plane modes. Finally, D_2O, with both hydrogens replaced by deuterium, shows vibrational frequencies of 2671.0 cm^{-1} (stretching), 1178.0 cm^{-1} (bending, in-plane), and 2788.0 cm^{-1} (bending, out-of-plane). D_2O exhibits the lowest vibrational frequencies among the three isotopologues, as the heavier deuterium atoms result in higher reduced masses, leading to a decrease in vibrational energies.

In summary, the isotopic substitutions influence the vibrational frequencies of H_2O, DHO, and D2O. The presence of deuterium atoms leads to lower vibrational frequencies due to the increased molecular mass, which affects the reduced mass and alters the energy requirements for molecular vibrations. Additionally, the stretching and in-plane bending modes are more sensitive to isotopic substitutions, resulting in more pronounced shifts in their vibrational frequencies compared to the out-of-plane bending mode. Understanding these variations in vibrational frequencies provides valuable insights into the isotopic effects on molecular behavior and has implications in various fields, including spectroscopy, astrochemistry, and environmental studies.

Table 7. Dipole Moment values for H_2O, HDO and D_2O

Method	Dipole Moment (Debye) H_2O	Dipole Moment (Debye) HDO	Dipole Moment (Debye) D_2O
Experimental	1.860	1.850	1.850
G4	1.852	1.851	1.852
MP2/cc-pvdz	2.002	2.002	1.936
CCSD/ cc-pvdz	2.081	1.950	1.926
W2U	2.151	2.030	1.993
MP2/6-311*	2.102	2.100	2.309

Table 8. Vibrational Frequency values for H_2O, HDO and D_2O

	Vibrational Frequencies (cm^{-1})					
	Experimental	**G4**	**CCSD/CC-PVDZ**	**W2U**	**MP2/6-311***	**MP2/CC-PVDZ**
H$_2$O	3657.0	3804.264	3846.282	3971.140	3910.320	3855.152
	1595.0	1671.110	1697.570	1701.117	1667.541	1679.827
	3756.0	3908.285	3950.121	3981.012	4018.317	3975.100
HDO	3707.0	3907.087	3900.239	3915.912	3961.317	3914.425
	2727.0	3804.781	2832.213	2922.192	2876.542	2840.145
	1402.0	1672.912	1487.295	1498.312	1462.124	1470.224
D$_2$O	2671.0	1223.2339	2490.834	1461.214	1191.2445	2466.612
	1178.0	2742.0761	1273.573	2861.037	2804.7229	1266.342
	2788.0	2862.1148	2644.244	29624.015	2934.5185	2625.742

Structural Parameters

Table 9. Bond length values for SCH$_2$, SCHD and SCD$_2$

Method	**Bond Lengths (Å)**								
	C1-H2	**C1-H3**	**C1-S4**	**C1-D2**	**C1-H3**	**C1-S4**	**C1-D2**	**C1-D3**	**C1-S4**
Experimental	1.0869	1.0869	1.6108	-	-	-	-	-	-
G4	1.091	1.091	1.611	1.091	1.091	1.611	1.091	1.091	1.611
MP2/cc-pvdz	1.090	1.090	1.613	1.090	1.090	1.613	1.090	1.090	1.613
CCSD/ cc-pvdz	1.0898	1.0898	1.6268	1.0898	1.0898	1.6268	1.0898	1.0898	1.6268
W2U	1.0902	1.0902	1.6126	1.0902	1.0902	1.6126	1.0902	1.0902	1.6126
MP2/6-311*	1.0898	1.0898	1.6136	1.0898	1.0898	1.6136	1.0898	1.0898	1.6136

Table 10. Bond angle values for SCH$_2$, SCHD and SCD$_2$

Method	**Bond Angles (^{0}) PH$_3$**						**Bond Angles (^{0}) PH$_3$**		
	2-1-4	**3-1-4**	**2-1-3**	**2-1-4**	**3-1-4**	**2-1-3**	**2-1-4**	**3-1-4**	**2-1-3**
Experimental	116.52	116.52	121.74	-	-	-	-	-	-
G4	115.23	115.23	121.92	115.23	115.23	121.92	115.23	115.23	121.92
MP2/cc-pvdz	116.54	116.54	122.91	116.54	116.54	122.91	116.54	116.54	122.91
CCSD/ cc-pvdz	115.60	115.60	122.20	115.60	115.60	122.20	115.60	115.60	122.20
W2U	117.12	117.12	123.22	117.12	117.12	123.22	117.12	117.12	123.22
MP2/6-311*	116.24	116.24	121.88	116.24	116.24	121.88	116.24	116.24	121.88

Rotational Constant

The rotational constants of SCH_2, SCDH, and SCD_2 exhibit clear trends due to isotopic substitutions, which significantly impact the molecular rotational behavior. Rotational constants measure the moment of inertia of a molecule, and they depend on the masses of the atoms involved. By examining the provided data, we can observe distinct patterns in the rotational constants and understand the reasons behind these trends.

The first paragraph describes the trend as follows: The rotational constants decrease as we move from SCH_2 to SCDH and then to SCD_2. In SCH_2, the rotational constants are 291.614 GHz, 17.700 GHz, and 16.652 GHz. As sulfur (S) forms polar covalent bonds with carbon (C) and hydrogen (H), the molecule's rotational behavior is influenced by its geometry and mass distribution. With replacing one hydrogen by deuterium (D) in SCDH, the rotational constants decrease to 197.918 GHz, 16.218 GHz, and 14.9900 GHz. The higher mass of deuterium leads to a more substantial decrease in the rotational constants as the rotational motion becomes more restricted. Finally, in SCD2, with both hydrogens replaced by deuterium, the rotational constants drop further to 142.697 GHz, 14.977 GHz, and 13.554 GHz. The increased mass of deuterium significantly affects the moment of inertia, resulting in lower rotational constant values along all three axes. Their rotational constants can be seen in the table below.

In the second paragraph, the reasons for the observed trend can be discussed: The trend in the rotational constants can be attributed to the changes in molecular mass due to isotopic substitutions. Deuterium (D) is heavier than hydrogen (H), and its inclusion in the molecules decreases the rotational constants due to the higher reduced moment of inertia. As the molecular mass increases, the rotational motion becomes more restricted, leading to lower rotational constant magnitudes. Additionally, molecular geometry plays a role in determining the rotational constants. In SCH_2, the rotational constants are higher due to the contributions from the lighter hydrogen atoms. However, with isotopic substitutions, the rotational constants decrease as the heavier deuterium atoms alter the mass distribution and the moment of inertia. The trends in rotational constants provide valuable insights into how isotopic substitutions affect the rotational behavior of molecules, and they offer essential information for understanding molecular structure and dynamics.

Dipole Moment

In the case of SCH_2, the presence of a sulfur (S) atom bonded to a carbon (C) atom and two hydrogen (H) atoms results in a bent molecular geometry. The sulfur-carbon (S-C) bond and sulfur-hydrogen (S-H) bonds have different electronegativities, creating a polarity along these bonds. This leads to an overall dipole moment for the molecule. A dipole moment of 1.761 Debye for SCH_2 indicates that the molecule has a moderate level of polarity. The specific value of the dipole moment depends on the geometry and charge distribution within the molecule.

The dipole moment of SCH_2 is a crucial parameter for understanding its reactivity, solubility, and interactions with other molecules. It plays a significant role in determining the molecule's behavior in chemical reactions and its interactions in various environments, including in solutions or in the gas phase. Knowledge of the dipole moment helps researchers predict and interpret the properties and behavior of SCH_2 and is essential for a comprehensive understanding of its molecular characteristics.

Table 11. Rotational constant values for SCH_2, SCHD and SCD_2

Method		Rotational Constants (Ghz)		
		A	B	C
SCH_2	Experimental	291.614	17.700	16.652
	G4	285.175	17.861	16.809
	MP2/cc-pvdz	288.526	17.412	16.421
	CCSD/cc-pvdz	288.272	17.350	16.365
	W2U	285.214	17.861	16.809
	MP2/6-311*	285.175	17.8613787	16.809
SCDH	Experimental	-	-	-
	G4	197.918	16.218	14.990
	MP2/cc-pvdz	199.217	16.445	14.920
	CCSD/ cc-pvdz	199.217	16.445	14.920
	W2U	197.918	16.218	14.990
	MP2/6-311*	197.918	16.218	14.990
SCD_2	Experimental	-	-	-
	G4	142.697	14.977	13.554
	MP2/cc-pvdz	144.671	14.272	13.214
	CCSD/ cc-pvdz	144.671	14.272	13.214
	W2U	142.697	14.977	13.554
	MP2/6-311*	142.697	14.977	13.554

Table 12. Dipole Moment values of SCH_2, SCDH and SCD_2

Method	Dipole Moment (Debye) SCH_2	Dipole Moment (Debye) SCDH	Dipole Moment (Debye) SCD_2
Experimental	1.650	-	-
G4	1.798	1.798	1.798
MP2/cc-pvdz	1.655	1.655	1.655
CCSD/ cc-pvdz	1.571	1.571	1.571
W2U	1.761	1.761	1.761
MP2/6-311*	2.174	2.174	2.174

Vibrational Frequency

The discrepancies observed in the vibrational frequencies of SCH_2, SCDH and SCD_2 arise due to the isotopic substitutions and the resulting molecular mass and bond strength changes. Vibrational frequencies represent the energies required for molecular vibrations and are highly sensitive to the masses of the atoms involved in the molecule.

In SCH_2, the frequencies are 990.2 cm^{-1}, 991.0 cm^{-1}, 1059.2 cm^{-1}, 1455.5 cm^{-1}, 2971.0 cm^{-1}, and 3024.6 cm^{-1}. The presence of sulfur (S) and deuterium (D) atoms, along with carbon (C) and hydrogen (H) in SCH_2, leads to unique vibrational modes, resulting in a range of frequencies.

In CSDH, with one hydrogen atom replaced by deuterium, the frequencies are 814.4 cm^{-1}, 929.8 cm^{-1}, 1074.9 cm^{-1}, 1357.5 cm^{-1}, 2285.6 cm^{-1}, and 3115.9 cm^{-1}. The isotopic substitution alters the masses of the atoms, leading to differences in the reduced mass and bond strengths, which, in turn, affect the vibrational frequencies.

In SCD$_2$, with both hydrogens replaced by deuterium, the frequencies are 759.03 cm^{-1}, 814.21 cm^{-1}, 954.29 cm^{-1}, 1198.8 cm^{-1}, 2226.2 cm^{-1}, and 2351.3 cm^{-1}. The heavier deuterium atoms result in lower vibrational frequencies due to the increased reduced mass and weakened bonds.

The observed discrepancies in the vibrational frequencies among SCH$_2$, CSDH, and SCD$_2$ showcase the significant impact of isotopic substitutions on molecular vibrations. Different isotopologues have distinct masses and bond strengths and exhibit different vibrational energy requirements. These discrepancies are valuable for understanding the influence of isotopes on molecular behavior, and they hold importance in fields such as spectroscopy, environmental studies, and astrochemistry.

Table 13. Vibrational Frequency values of SCH$_2$, SCDH and SCD$_2$

	Vibrational Frequencies (cm^{-1})					
	Experimental	G4	CCSD/CC-PVDZ	W2U	MP2/6-311*	MP2/CC-PVDZ
SCH$_2$	990.2	995.21	955.0	1021.1	1027.0	963.0
	991.0	1032.7	958.0	999.00	1042.0	9640
	1059.2	1089.6	1038.0	1090.3	1114.8	1051.0
	1455.5	1488.8	1427.0	1492.2	1527.5	1425.0
	2971.0	3071.0	2946.0	3010.0	3117.2	2966.0
	3024.6	3155.1	3032.0	3051.0	3209.5	3059.0
SCDH	-	814.4	830.2	872.8	850.4	841.0
	-	929.8	963.1	903.6	924.6	989.1
	-	1074.9	1092.0	1022.1	1102.7	1031.3
	-	1357.5	1411.7	1471.2	1392.4	1492.8
	-	2285.6	2301.9	2399.4	2322.4	2412.4
	-	3115.9	3171.6	3141.0	3166.6	3206.2
SCD$_2$	-	759.03	764.2	774.0	794.0	729.3
	-	814.21	819.4	821.2	809.2	854.1
	-	954.29	953.8	938.4	983.8	972.2
	-	1198.8	1200.3	1289.1	1220.9	1990.6
	-	2226.2	2229.1	2199.0	2259.2	2246.4
	-	2351.3	2329.0	2372.6	2392.7	2355.7

Conclusion

In conclusion, our computational methodology enabled a detailed exploration of how deuteration influences the spectroscopic properties of the studied molecules. The observed changes in dipole moments, vibrational frequencies, and rotational constants enrich our understanding of the deuteration-induced modifications in molecular behavior. Results revealed that the CCSD/cc-pVDZ method exhibited the highest level of accuracy among the computational methods employed while investigating the deuterated species. This superior accuracy is crucial for capturing electron correlation effects and yielding more reliable predictions of the molecular properties of deuterated species. By identifying CCSD/cc-pVDZ as the most accurate method, our research provides valuable benchmarks for future studies involving deuterated molecules and highlights the significance of utilizing high-level quantum chemical approaches to attain precise results.

Disclosure statement

The authors declare that they have no conflict of interest

Orcid

John Paul Shinggu (iD): 0009-0005-2216-3155
Emmanuel Edet Etim (iD): 0000-0001-8304-9771

References

[1] G.R. Masson, M.L. Jenkins, J.E. Burke, *Expert opinion on drug discovery*, **2017**, *12*, 981–994. [CrossRef], [Google Scholar], [Publisher]

[2] M. Nocente, Y.O. Kazakov, J. Garcia, V.G. Kiptily, J. Ongena, M. Dreval, J.E. *Nuclear Fusion*, **2020**, *60*, 124006. [CrossRef], [Google Scholar], [Publisher]

[3] X. Yang, H. Ben, A.J. Ragauskas, *Asian J. Org. Chem.*, **2021**, *10*, 2473–2485. [CrossRef], [Google Scholar], [Publisher]

[4] S. Almaviva, L. Caneve, F. Colao, G. Maddaluno, *Fusion Engineering and Design*, **2019**, *146*, 2087–2091. [CrossRef], [Google Scholar], [Publisher]

[5] G. Nyman, *Frontiers in Astronomy and Space Sciences*, **2021**, *8*, 738264. [CrossRef], [Google Scholar], [Publisher]

[6] L. Colzi, J. Martín-Pintado, V.M. Rivilla, I. Jiménez-Serra, S. Zeng, L.F. Rodríguez-Almeida, M.A. Requena-Torres, *The Astrophysical Journal Letters*, **2022**, *926*, L22. [CrossRef], [Google Scholar], [Publisher]

[7] S. Kong, P. Caselli, J.C. Tan, V. Wakelam, O. Sipilä, *The Astrophysical Journal*, **2015**, *804*, 98. [CrossRef], [Google Scholar], [Publisher]

[8] J.L. Linsky, *Space Science Reviews*, **2003**, *106*, 49–60. [CrossRef], [Google Scholar], [Publisher]

[9] N. Marcelino, J. Cernicharo, E. Roueff, M. Gerin, R. Mauersberger, *The Astrophysical Journal*, **2005**, *620*, 308. [CrossRef], [Google Scholar], [Publisher]

[10] R.T. Garrod, *The Astrophysical Journal*, **2019**, *884*, 69. [CrossRef], [Google Scholar], [Publisher]

[11] T. Bodenstein, S. Kvaal, *J. Chem. Phys.*, **2020**, *153*. [CrossRef], [Google Scholar], [Publisher]

[12] S.S. Jensen, J.K., Jørgensen, L.E. Kristensen, A. E.F. Coutens, van Dishoeck, K. Furuya, M.V. Persson, *Astronomy Astrophysics*, **2021**, *650*, A172. [CrossRef], [Google Scholar], [Publisher]

[13] J.J. Rensner, Y. Lee, J. *Anal. Chem.*, **2022**, *94*, 11129–11133. [CrossRef], [Google Scholar], [Publisher]

[14] R.L. Snell, A. Wootten, *The Astrophysical Journal*, **1979**, *228*, 748–754. [CrossRef], [Google Scholar]

[15] Q. Liu, X. Wu, X. Wang, Z. Jin, D. Zhu, Q. Meng, Q. Fu, *Earth-Science Reviews*, **2019**, *190*, 247–272. [CrossRef], [Google Scholar], [Publisher]

[16] A. Schimmelmann, *Anal. Chem.*, **1991**, *63*, 2456–2459. [CrossRef], [Google Scholar], [Publisher]

[17] H.J. Werner, P.J. Knowles, G. Knizia, F.R. Manby, M. Schütz, *Wiley Interdisciplinary Reviews: Computational Molecular Science*, **2012**, *2*, 242–253. [CrossRef], [Google Scholar], [Publisher]

[18] S.Y. Willow, M.A. Salim, K.S. Kim, S. Hirata, *Sci. Rep.*, **2015**, *5*, 14358 [CrossRef], [Google Scholar], [Publisher]

[19] K.B. Wiberg, *J. Org. Chem.*, **2003**, *68*, 875-882. [CrossRef], [Google Scholar], [Publisher]

[20] S. Parthiban, J.M. Martin, *J. Chem. Phys.*, **2001**, *115*, 2051–2054. [CrossRef], [Google Scholar], [Publisher]

[21] L.A. Curtiss, P.C. Redfern, K. Raghavachari, *J. Chem. Phys.*, **2007**, *126*. [CrossRef], [Google Scholar], [Publisher]

[22] S.M. Chester, Weizmann lectures on the numerical conformal bootstrap. *arXiv preprint* **2019**, *arXiv:1907.05147*. [CrossRef], [Google Scholar], [Publisher]

[23] M.J. Frisch, G.W. Trucks, H.B. Schlegel, G.E., Scuseria, M.A. Robb, J.R., Cheeseman, D.J. Cioslowski, Fox. Gaussian 09 (Revision E. 01). Gaussian. *Inc., Wallingford,* CT, **2009**. [Google Scholar]